IEEE Access
Multidisciplinary | Rapid Review | Open Access Journal

Received 19 December 2023, accepted 2 January 2024, date of publication 8 January 2024,
date of current version 17 January 2024.

*Digital Object Identifier 10.1109/ACCESS.2024.3351185*

RESEARCH ARTICLE

# Broadband Circularly Polarized Printed Crossed-Dipole Antenna and Its Arrays for Cellular Base Stations

**MEHDI SEFIDI[1], CHANGIZ GHOBADI[1], JAVAD NOURINIA[1], (Senior Member, IEEE), AND RAHIM NADERALI[2]**

[1]Department of Electrical Engineering, Urmia University, Urmia 57561-51818, Iran
[2]Department of Physics, Faculty of Sciences, Urmia University, Urmia 57561-51818, Iran

Corresponding author: Changiz Ghobadi (ch.ghobadi@urmia.ac.ir)

**ABSTRACT** This study presents and investigates broadband circularly polarized (CP) printed crossed dipole antenna and its arrays. The proposed antenna comprises a pair of crossed fan-shaped dipoles, two kinds of parasitic elements, and a reflector with two vertical sidewalls. A three-quarter circular phase shifter connected to the fan-shaped arms of this antenna allows it to radiate CP waves owing to the excitation of the arms and the creation of sequential phases. The significant contribution of this study is the creation of electromagnetic coupling between crossed fan-shaped dipoles and parasitic elements to improve the purity of CP radiation and increase the axial ratio (AR) bandwidth. The proposed antenna has upgraded into 4-element and 8-element array models as cellular base station antennas for PCS/DCS/UMTS systems. Experiments indicate that the proposed CP antenna achieves an impedance bandwidth of 57% (1.47-2.65 GHz) for VSWR $< 2$, an AR bandwidth of 33% (1.65-2.3 GHz) for AR $< 3$ dB, and a gain of 7.8-8.7 dB. The implemented arrays of $1 \times 4$ and $1 \times 8$ arrangement achieve peak gains of 13.2 and 16.1 dB, respectively. The horizontal half-power beam widths (HPBWs), horizontal axial ratio beam widths (ARBWs), and front-to-back ratios (FBRs) for the antenna arrays are approximately $64° \pm 3°$, $> 90°$, and $> 25$ dB, respectively.

**INDEX TERMS** Antenna array, axial ratio, base station, circularly polarized, crossed-dipole.

## I. INTRODUCTION

With the rapid growth of mobile cellular networks, there is a tremendous demand for high-performance antennas with maximum coverage at base stations [1], [2]. Dual-polarized antennas use polarization-diversity technology to provide high-quality mobile communication services [2]. Owing to the increased channel capacity and reduced multipath fading, linearly polarized (LP) antennas with $\pm 45°$ dual slant polarization have been set up as standard base station antennas to provide mobile communication services [3]. Therefore, Researchers have attempted to design and introduce different structures of this type of antenna for base transceiver station (BTS) applications, including crossed-dipole antennas [4], [5], [6], [7], [8], [9], [10], patch antennas [11], [12], [13], magneto-electric dipole antennas [14], [15], [16] and slot antennas [17]. The ease of structural modification of dual-polarized ($\pm 45°$) crossed dipole antennas can satisfy the requirements of BTS antennas, such as low cost, simple assembly high, front-to-back, high isolation, broad impedance bandwidth, and desirable beam width for the cell sector design [1], [2], [3], [4], [5], [6], [7], [8], [9], [10]. Compared to other categories of base station systems, these antennas are in high demand. Engineers have recently employed dipole antennas in various approaches to create circularly polarized antennas for wireless communication systems [18], tuning the length of two orthogonal dipoles independently to generate dual-CP radiation for WLAN/WiMAX applications [19], using trident-shaped dipoles for three operating WLAN bands [20], employing a miniaturizing technique and two kinds of dipoles to achieve dual CP bands for radio frequency identification RFID

The associate editor coordinating the review of this manuscript and approving it for publication was Hassan Tariq Chattha.

readers [21], designing a tapered meander line CP-crossed dipole antenna for RFID applications [22], and introducing a compact multi-band CP dipole antenna, integrating both positioning techniques for handheld RFID and GPS applications [23]. Other pioneering approaches focused on feeding CP crossed-dipole antennas tailored for GPS applications, such as swallow-tailed feed-strip [24], unequal power network [25], and combination of printed balun and branch-line coupler [26]. Owing to the increasing attention of researchers in UWB systems, a diverse range of CP UWB dipole antennas have recently been documented in research papers, such as an asymmetric elliptical-shaped dipole array antenna [27] and cavity-backed crossed-dipole antenna [28]. With the advancement of wireless systems technology, the demand for employing CP dipole antennas in the sub-6 GHz frequency band has increased, such as CP Compact planar magneto-electric dipole-like antenna [29]. Owing to the desirable performance of CP dipole antennas in the proposed application systems and recent progress in the development of mobile communication services, there is a pressing need to employ these antennas in base station applications. Employing CP antennas at cellular base stations offers advantages over linearly polarized antennas. Compared with linearly polarized antennas, CP antennas provide better coverage and penetration through obstacles. Because the signal can maintain its polarization, it can propagate more effectively in urban environments with many obstacles. A CP antenna can decrease signal interference from neighboring base stations. This phenomenon occurs because CP signals excel at distinguishing between signals with different polarizations, thereby reducing the chances of interference. CP antennas increase cellular network capacity by utilizing spectrum efficiently. Therefore, the CP operation uses both right-hand and left-hand polarizations, doubling the available bandwidth. By designing a fan-shaped CP-crossed dipole antenna and its linear arrays, this study has made a valuable contribution in this direction, covering personal communications service (PCS: 1.85–1.99 GHz), digital cellular system (DCS: 1.71–1.88 GHz), and universal mobile telecommunications service (UMTS: 1.92–2.17 GHz) frequency bands for base stations. In the proposed antenna, the orientation of the fan-shaped arms, combined with the three-quarter circular phase shifter, enables the generation of sequential phases, resulting in CP excitation modes that create the conditions for CP radiation. The electromagnetic coupling effect between the parasitic elements and fan-shaped arms improves the CP characteristics (AR bandwidth and purity of CP radiation). Using the characteristics of circular polarization in cellular communications improves performance in terms of reduced multipath fading, reduced polarization mismatch losses, improved coverage, better penetration, and increased capacity and efficiency. In next-generation communication systems to ensure the connection between 4G/5G smartphones (designed at the sub-6 GHz long-term evolution (LTE) band) [30], [31] and network infrastructure, the array models of the proposed antenna contribute to achieving higher

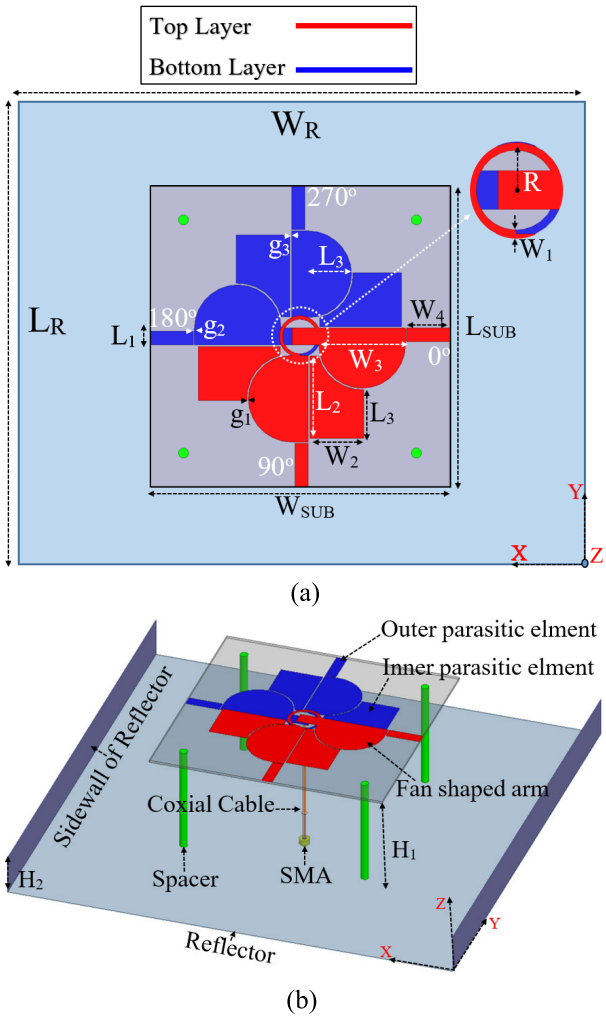


**FIGURE 1.** Geometry of the proposed antenna. (a) top view, and (b) 3-D view.

data rates through the self-diplexing technique in [32] for frequency tuning, increased spatial diversity, and multipath mitigation in the form of upgrading the antenna structure and updating its capabilities.

## II. ANTENNA DESIGN

Fig. 1 illustrates the configuration of the proposed cross-dipole antenna. Two adjacent fan-shaped arms on the same layer connected to a three-quarter circular phase shifter with a length of $\lambda e/4$ ($\lambda e$ is the effective wavelength at the center frequency) are etched on both sides of a dielectric substrate (FR4, $\varepsilon_r = 4.4$) with a thickness of 0.8 mm to excite the CP radiation wave. The proposed crossed fan-shaped dipole antenna was designed to achieve better CP performance using two parasitic elements with different shapes and through capacitive coupling. Fig. 1 shows the placement of inner boot-shaped parasitic elements near the inner edges of the fan-shaped arms and outer strip-shaped parasitic elements near the outer edges of the fan-shaped arms. A 50 Ω coaxial cable feeds the proposed antenna by soldering the inner and

**TABLE 1. Physical dimensions of the proposed antenna.**

| Parameter | Value (mm) | Parameter | Value (mm) |
|---|---|---|---|
| $L_{Ref}$ | 172.2 | $W_1$ | 1 |
| $W_{Ref}$ | 172.2 | $W_2$ | 16 |
| $L_{Sub}$ | 90 | $W_3$ | 26 |
| $W_{Sub}$ | 90 | $W_4$ | 12.9 |
| $L_1$ | 4 | $H_1$ | 40 |
| $L_2$ | 24.6 | $H_2$ | 15 |
| $L_3$ | 14.5 | $g_1$ | 0.5 |
| $L_4$ | 13 | $g_2$ | 0.4 |
| R | 5.7 | $g_3$ | 0.5 |

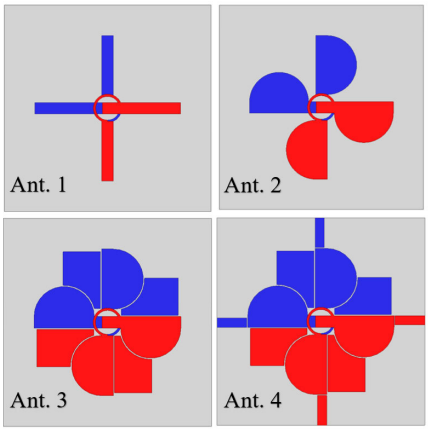


**FIGURE 2. Evolution stages of the proposed antenna.**

outer conductors of the coaxial cable to the upper and lower curved phase shifter rings, respectively. The phase-shifter ring creates a 90-degree phase difference between adjacent fan-shaped arms on the same layer, enabling CP operation. A metallic reflector with two sidewalls is placed below the proposed crossed dipole antenna at the distance of H1 to create a CP unidirectional radiation pattern with a half-power beam width (HPBW) of approximately 65° in the horizontal plane (x-z plane) by adjusting the height of the side walls. Table 1 lists all dimensional parameters of the proposed antenna.

Fig. 2 shows the evolution stages of the proposed antenna. Ant. 1 consists of two orthogonal straight dipoles; Ant. 2 is a fan-shaped crossed dipole antenna; Ant. 3 is a fan-shaped crossed dipole antenna with two pairs of inner parasitic elements; and Ant. 4 consists of Ant. 3; and four outer strip-shaped parasitic elements. The information presented in Fig. 3 indicates that Ant. 1 has a narrow impedance bandwidth with undesirable AR bandwidth (based on the 3 dB criterion) and produces a CP mode within a lower frequency range, Ant. 2 only contains a single AR resonance point at 1.75 GHz with an improvement of impedance bandwidth at lower frequencies and the previous CP mode moves towards the beginning of the band with higher purity, two pairs of inner boot-shaped parasitic elements are added in Ant. 3 to improve impedance bandwidth and produces excess CP modes in the middle and high frequencies. For Ant. 4 with

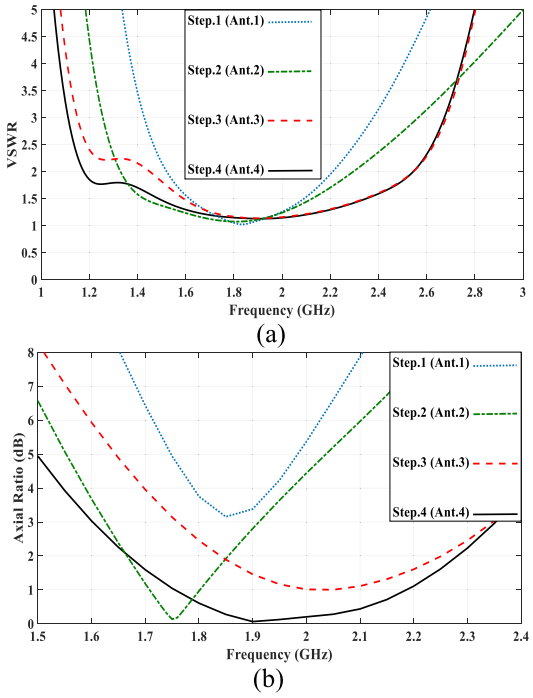


**FIGURE 3. Simulated VSWR and AR curves for Ant. 1-4. (a) VSWR, and (b) AR.**

**TABLE 2. Optimized values of elements employed in the proposed antenna circuit model.**

| Parameter | Value (nH) | Parameter | Value (PF) |
|---|---|---|---|
| $L_1$ | 5.095 | $C_1$ | 1.099 |
| $L_2$ | 10.095 | $C_2$ | 0.639 |
| $L_3$ | 1.599 | $C_3$ | 10.09 |
| $L_4$ | 8.092 | $C_4$ | 8.092 |
| $L_5$ | 6.094 | $C_5$ | 3.097 |
| $L_6$ | 10.09 | | |
| $L_7$ | 4.096 | | |

inner and outer parasitic elements, the impedance bandwidth at lower frequencies and the Purity of CP mode in the whole frequency band are significantly improved compared to the previous antennas.

Fig. 4 (a) shows the equivalent circuit model of Ant. 4. The ADS software fine-tuned and determined all values of the circuit design parameters. As shown in Fig. 4, each circuit parameter is equivalent to part of the proposed dipole antenna structure. Fig. 4 (b) demonstrates a close alignment between the S-parameter results of Ant. 4 derived from HFSS software and those acquired using the circuit model. Table 2 lists the optimized values of the elements employed in the proposed antenna circuit model.

Equations (1) and (2) evaluate the S-parameter curve of the circuit model, where $|\Gamma|$ and $Z_{in}$ is the reflection coefficient and antenna input impedance, respectively [33].

$$|\Gamma| = \frac{Z_{in} - Z_{Terminal}}{Z_{in} + Z_{Terminal}}, Z_{Terminal} = 50\Omega, R_1 = R_{in} = 57.04\Omega \quad (1)$$

$$S_{11}(dB) = 20\log(|\Gamma|) \quad (2)$$

**TABLE 3.** Performance comparison between some references and proposed antennas.

| Ref. | Size ($mm^3$) | BW (GHz) | Peak Gain (dB) | Polarization mode | Application |
|---|---|---|---|---|---|
| [5] | 170×170×35.5 | 1.4-2.8 (VSWR < 1.5) | 9.6 | LP/±45° | BTS |
| [6] | 140×140×34 | 1.7-2.7 (VSWR < 1.5) | 8.8 | LP/±45° | BTS |
| [8] | 300×145×34.7 | 1.63-2.95 (VSWR < 1.5) | 8.8 | LP/±45° | BTS |
| [9] | 150×150×32.5 | 1.7-2.9 (VSWR < 1.5) | 7 | LP/±45° | BTS |
| [20] | 72×72×17.54 | 2.4/5.2/5.8 ($S_{11}$ < -10 dB) | 6.8/6.6/6.8 | CP | WLAN |
| [21] | 85×85 ×1.6 | (0.871-1.297), (2.16-2.8) ($S_{11}$ < -10 dB) | 0.66/2.6 | CP | RFID |
| [25] | 140×140×50 | 1.01-2.01 ($S_{11}$ < -10 dB) | 7.1 | CP | GPS |
| [28] | 124×124×28 | 1.67-7.26 ($S_{11}$ < -10 dB) | 12.2 | CP | UWB |
| [29] | 36×36×3 | 6.15-7.01 ($S_{11}$ < -10 dB) | 4.5 | CP | Sub-6 GHz |
| Single (This work) | 172.2×172.2×40 | 1.64-2.4 (VSWR < 1.5) | 8.7 | CP | BTS |
| 1×4 Array (This work) | 400×172.2×40 | 1.36-2.2 (VSWR < 1.5) | 13.2 | CP | BTS |
| 1×8 Array (This work) | 808×172.2×40 | 1.33 - 2.08 (VSWR < 1.5) | 16.1 | CP | BTS |

## III. PARAMETRIC STUDY AND PERFORMANCE PRINCIPLE OF THE ANTENNA

This study conducted a parametric investigation to describe the influence of effective parameters on the AR bandwidth and purity of CP radiation. Thus, the effects of the middle radius and thickness of the three-quarter circular phase shifter (R and $W_1$) and the distance between the reflector and radiator element ($H_1$) on the CP characteristics were analyzed using HFSS software, and their values were optimized. Fig. 5 presents the AR for different sizes of R, $W_1$, and $H_1$, and a desirable AR bandwidth with high CP purity is achieved when these critical parameters are chosen as 5.7, 1, and 40 mm, respectively.

Fig. 6 shows the distributions of the simulated surface current density of the proposed crossed dipole antenna at 1.8 GHz for different time points: t=0, T/4, T/2, and 3T/4. The direction of the vector current at t=0 is orthogonal to that at t=T/4. Additionally, there is a similarity in the surface current intensity amplitude at the two times, and a similar mechanism for next time points (t=T/2 and t=3T/4) is describable, resulting in the CP radiation. The proposed antenna can generate left-hand circularly polarized (LHCP) waves at 1.8 GHz since the vector surface current rotates clockwise from t=0 to t=3T/4.

## IV. SIMULATED AND MEASURED RESULTS

The proposed antenna's simulated normalized radiation patterns at different frequencies ranging from 1.7 to 2.3 GHz, with HPBW values of about 65° and FBR of approximately 18 dB, are depicted in Fig. 7. To some extent, they meet the required standards for base station antennas. Fig. 8 shows photographs of the fabricated sample of the proposed antenna and its experimental setup. Fig. 9 depicts a side-by-side comparison of the simulated and measured VSWR curves for the proposed crossed-dipole antenna. Both curves show an acceptable agreement. The VSWR bandwidth of the proposed antenna was measured from 1.47 GHz to 2.65 GHz (57%) for VSWR < 2, where VSWR < 1.5 (1.64 - 2.4 GHz). Fig. 10 shows the gain and AR performance of the proposed antenna. The measured AR bandwidth is from 1.65 GHz to 2.3 GHz (33%) for an AR < 3 dB, and the minimum AR point is at 1.9 GHz. The measured gain is between 7.8 and 8.7 dB from 1.5 to 2.4 GHz. Fig. 11 shows the unidirectional radiation patterns of the proposed crossed-dipole antenna at frequencies of 1.7 and 1.9 GHz. There is an acceptable similarity between the simulated and measured radiation patterns.

## V. FOUR-ELEMENT CP CROSSED-DIPOLE ANTENNA ARRAY AND ITS RESULTS

Increasing the gain of the proposed crossed-dipole antenna to a high level is necessary for its use in base station systems. Extending this to an array antenna serves this purpose. Thus, a 4-element array and an 8-element array were developed based on the proposed antenna element. Fig. 12 shows the configuration of the 4-element array antenna. The array antenna consists of two FR4 substrates ($\varepsilon_r = 4.4$) (top and bottom)

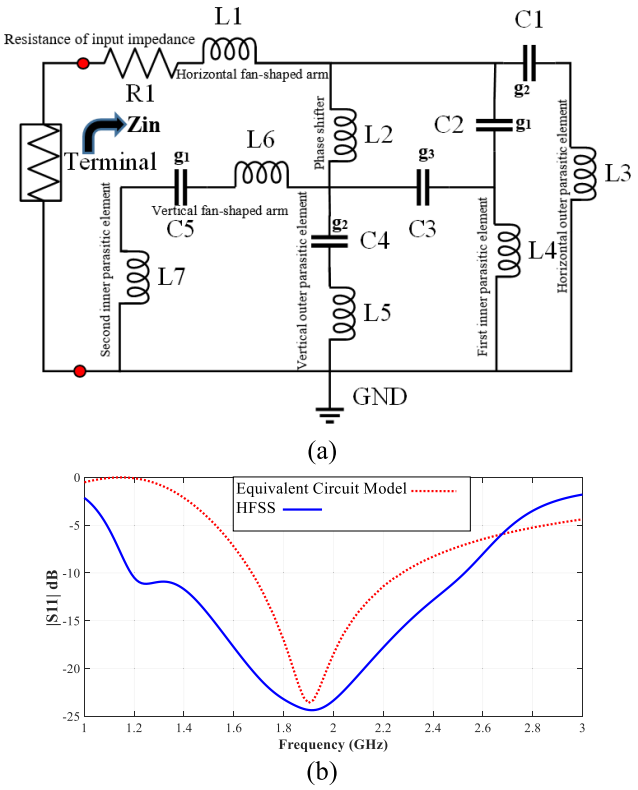


**FIGURE 4.** (a) Equivalent circuit model of Ant. 4. (b) |S11| of Ant.4 using HFSS and the equivalent circuit model.

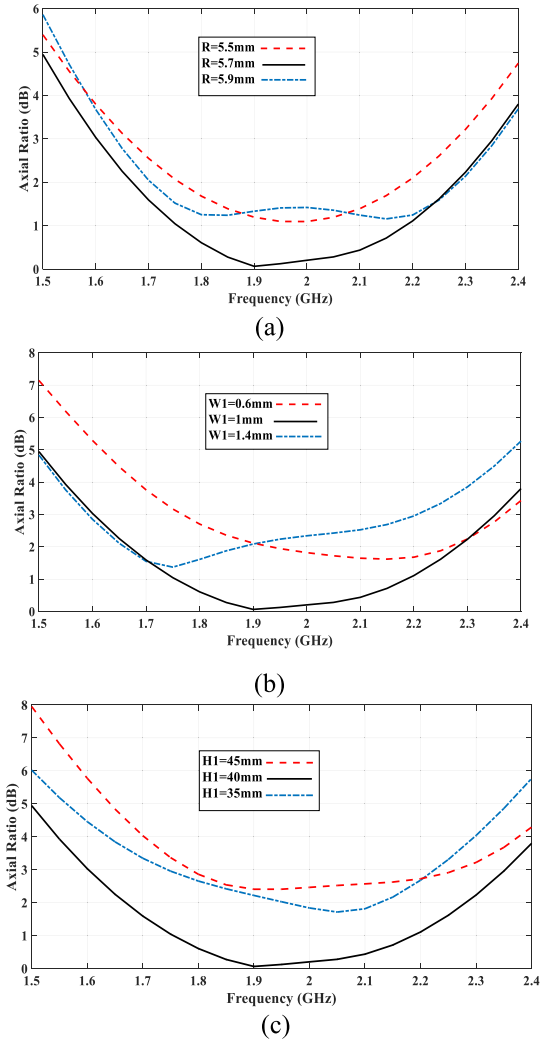


**FIGURE 5.** Effects of various parameters on AR. (a) R, (b) $W_1$, and (c) $H_1$.

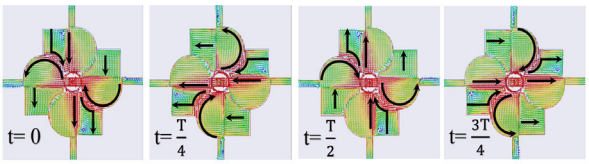


**FIGURE 6.** Simulated current vectors of the proposed CP antenna at 1.8 GHz.

with equal sizes of 400 × 172.2 mm2 and thicknesses of 0.8 and 1 mm, respectively. Four identical 50 Ω coaxial cables establish the connection between the two proposed substrates. The top substrate houses the four proposed antenna elements, whereas the bottom substrate accommodates the antenna feeding network with a U-shaped reflector. A flat plane reflector with two sidewalls (U-shaped reflector) was employed to achieve high-level gain and adjust the HPBW in the x-z plane. The distance between the centers of adjacent elements was 102 mm. Three T-junction power dividers were used in the feeding network to split the power equally and excite the 4-element array antenna through coaxial lines. The T-junction power divider consists of a 50 Ω input line with $W_0$ =1.9 mm, two 50 Ω out pout lines, and a transmission line in the form of a quarter-wave impedance transformer with a length of λe/4 (λe is the effective wavelength at the center frequency) and impedance of 35 Ω with $W_1$ =3.3 mm for impedance matching.

Fig. 13 (a) displays photographs of the test condition for the 4-element CP crossed dipole antenna array fabricated model. Fig. 13 (b) presents the simulated and measured VSWR results for the proposed 4-element array. The slight difference between the results was due to fabrication errors and instrument calibration. The measured impedance bandwidth of the proposed antenna array operates from 1.26 GHz to 2.5 GHz (66%) for VSWR < 2, in which VSWR < 1.5 (1.36 - 2.2 GHz), as shown in Fig. 13 (b). Fig. 14 (a) shows the simulated and measured AR and the gain results of the 4-element array. The slight discrepancies between the simulated and measured results were due to measurement errors. The measured (3 dB) AR bandwidth is 39% (1.55-2.3 GHz), and the measurement gain is between 12.1 and 13.2 dB from 1.4 GHz to 2.4 GHz. Fig. 14 (b) shows the two required functional specifications of the base station antennas (HPBW ∼ 65°± 10°, ARBW ∼ 100°, and FBR ≥ 25 dB) for the proposed array. According to the simulated results in the figure, this array fulfills the requirements mentioned earlier with HPBW∼ 63°± 5°, ARBW > 90°, and FBR between

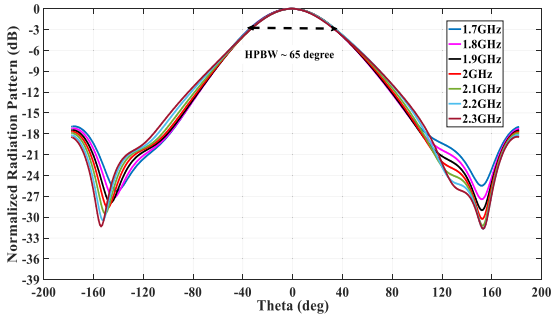


**FIGURE 7.** Simulated normalized radiation patterns of the proposed CP antenna at different frequencies.

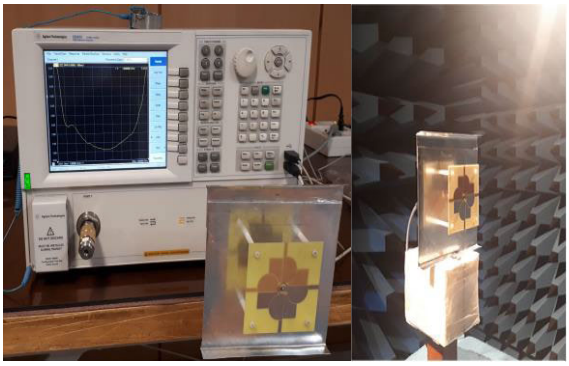

**FIGURE 8.** Fabricated prototype of the proposed antenna.

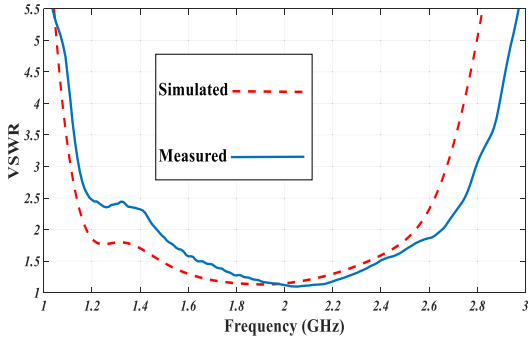


**FIGURE 9.** Simulated and measured VSWR of the proposed antenna.

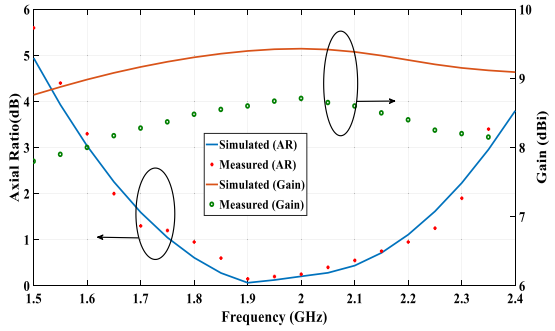


**FIGURE 10.** Simulated and measured axial ratio and gain of the crossed-dipole antenna.

25 dB and 32 dB in the frequency range of 1.7 GHz to 2.2 GHz.

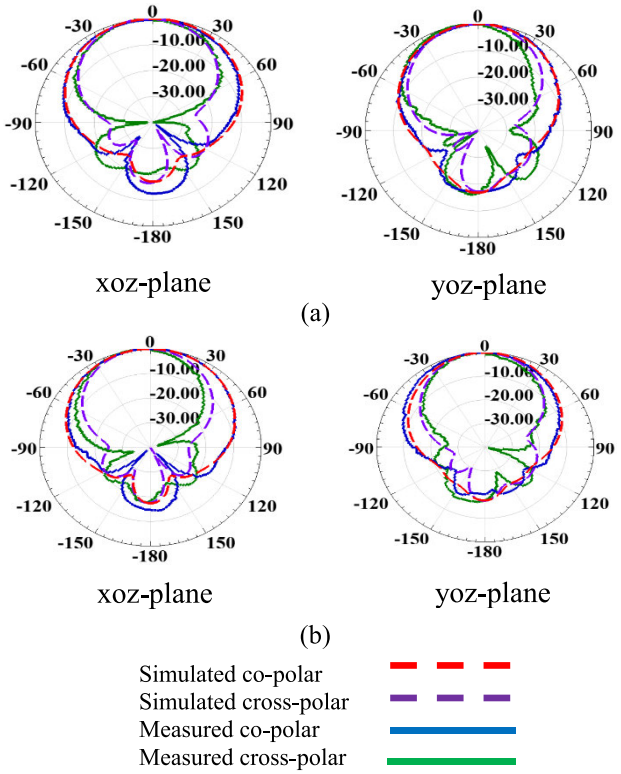


**FIGURE 11.** Radiation patterns of the crossed-dipole antenna at (a) 1.7 GHz, and (b) 1.9 GHz.

The simulated and measured radiation patterns in Fig. 15 serve to validate the results presented in the previous figure. At 1.7 GHz and 1.9 GHz, the antenna achieves measured HPBWs of approximately 67° and 61° in the horizontal plane, respectively. In addition, the measured FBR values are about 25 dB and 27 dB at frequencies of 1.7 GHz and 1.9 GHz, respectively.

## VI. EIGHT-ELEMENT CP CROSSED-DIPOLE ANTENNA ARRAY AND ITS RESULTS

The proposed 4-element array antenna is upgraded to an 8-element array to meet the base station standards for the gain parameter value. Fig. 16 shows a detailed schematic of an 8-element circularly polarized crossed dipole antenna array with a 1-8 feeding network. The feeding network structure employs seven T-junction power dividers to transmit and distribute equal power among the radiation elements through coaxial cables.

Fig. 17 (a) illustrates the experimental testing procedure for the prototype of an 8-element CP crossed dipole antenna array. Fig. 17 (b) presents the simulated and measured VSWR plots of the proposed 8-element antenna array. The array antenna achieves the measurement results of the impedance bandwidth from 1.29 GHz to 2.29 GHz %56 and 1.38 GHz to 2.7 GHz %12.6 for VSWR $<$ 2, in which VSWR $<$ 1.5 (1.33 - 2.08 GHz). Fig. 18 (a) shows the AR and gain results of the proposed antenna array. The measured (3 dB)

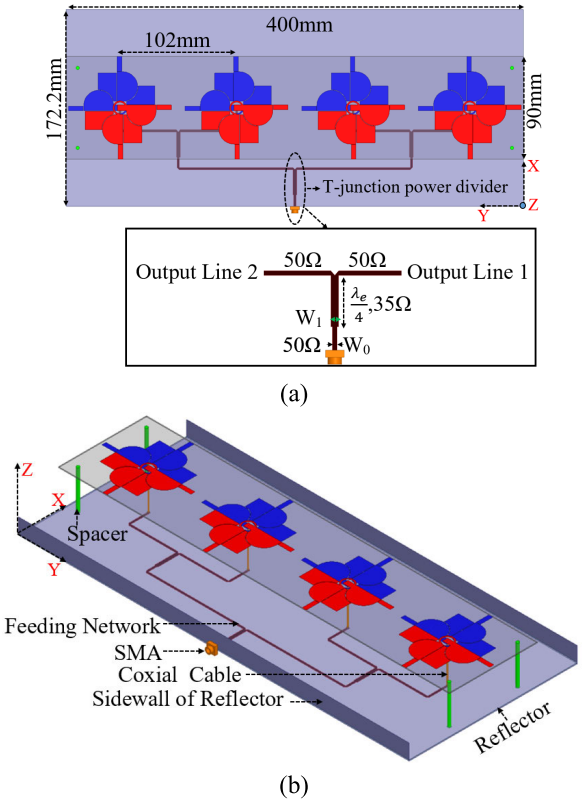


**FIGURE 12.** Schematic of a 4-element CP dipole array antenna. (a) top view, and (b) 3-D view.

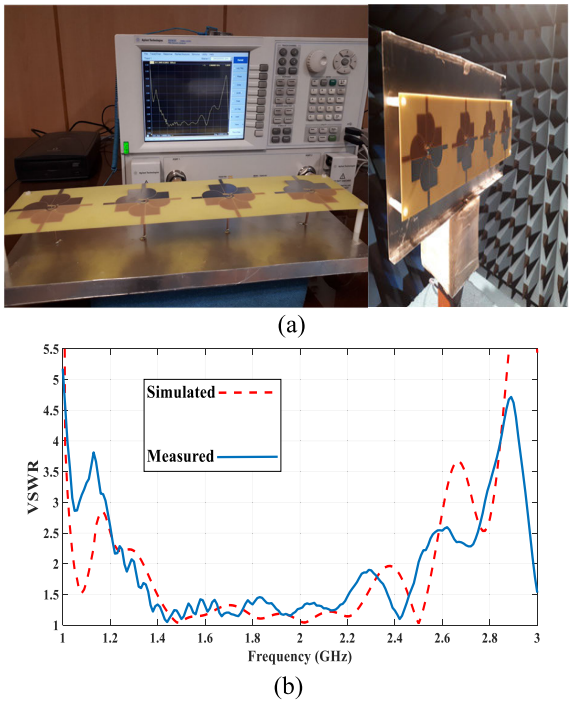


**FIGURE 13.** (a) Fabricated model of the 4-element CP dipole array antenna and its test setup. (b) Simulated and measured VSWR of the 4-element antenna array.

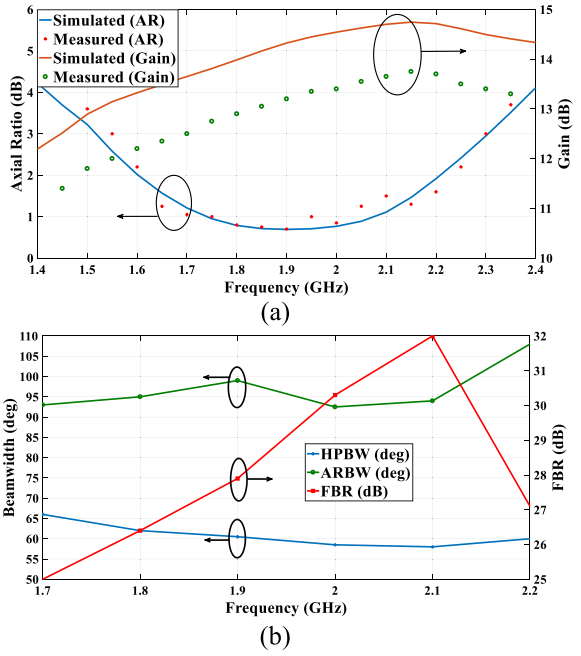


**FIGURE 14.** (a) Simulated and measured axial ratio and gain of the 4-element antenna array. (b) Simulated HPBW, ARBW, and FBR of the 4-element antenna array.

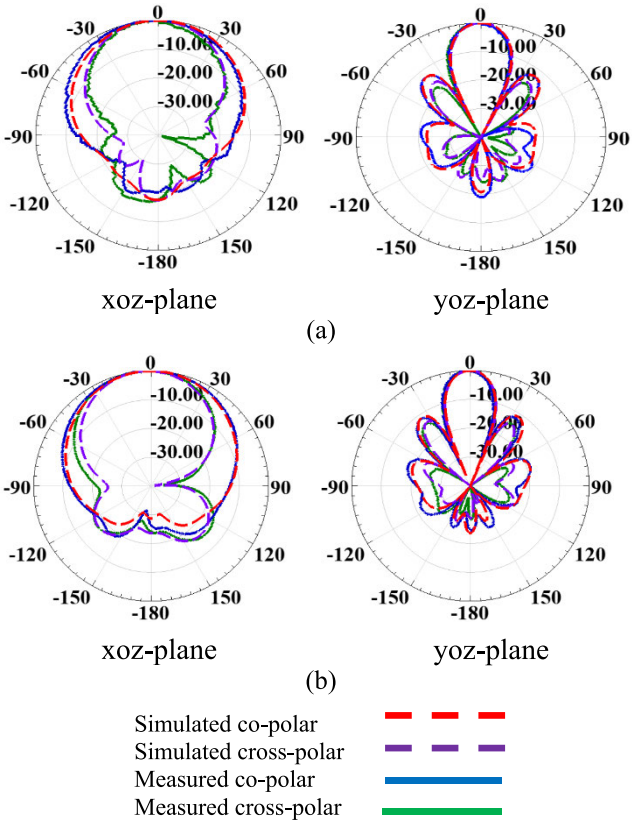


**FIGURE 15.** Radiation patterns of the 4-element antenna array at (a) 1.7 GHz, and (b) 1.9 GHz.

AR bandwidth is 42% (1.5 - 2.3 GHz), and the maximum measurement gain is 16.1 dB at 2.15 GHz. Fig. 18 (b) shows the simulated HPBW, ARBW, and FBR of the 8-element CP crossed dipole antenna array. The HPBW in the x-z plane

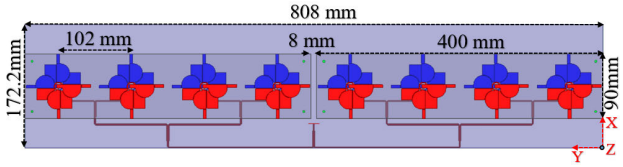


**FIGURE 16.** Schematic of an 8-element CP dipole array antenna.

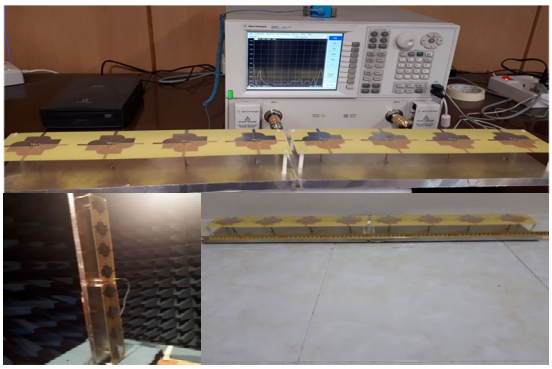

(a)

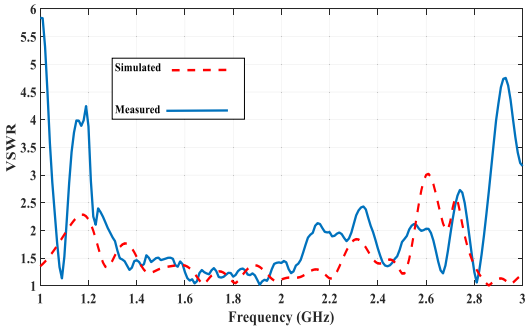


(b)

**FIGURE 17.** (a) Prototype of the 8-element CP dipole array antenna and its experimental testing procedure. (b) Simulated and measured VSWR of the 8-element antenna array.

is 62.5° ± 5.5°, ARBW in the x-z plane is more than 90°, and FBR is between 26 dB and 33 dB in the frequency range of 1.7 GHz to 2.2 GHz. Fig. 19 demonstrates the stable directional radiation patterns of the 8-element antenna array for frequencies of 1.7 GHz and 1.9 GHz with the back-lobe radiation level of less than -20 dB and side-lobe level (SLL) of about -15 dB without the grating lobe. The measured azimuth HPBWs of the proposed 8-element array at measurement frequencies (1.7 GHz and 1.9 GHz) are about 66° and 62°, respectively. Thus, this 8-element CP antenna array is a suitable candidate for cellular base station applications. Table 3 shows a performance comparison between the proposed antennas and some references mentioned in this article. It is clear that none of the base station antennas in [5], [6], [7], [8], and [9] benefit from the CP advantages. Other applications of wireless systems, excluding base stations, use the remaining crossed dipole antennas with CP characteristics in this table.

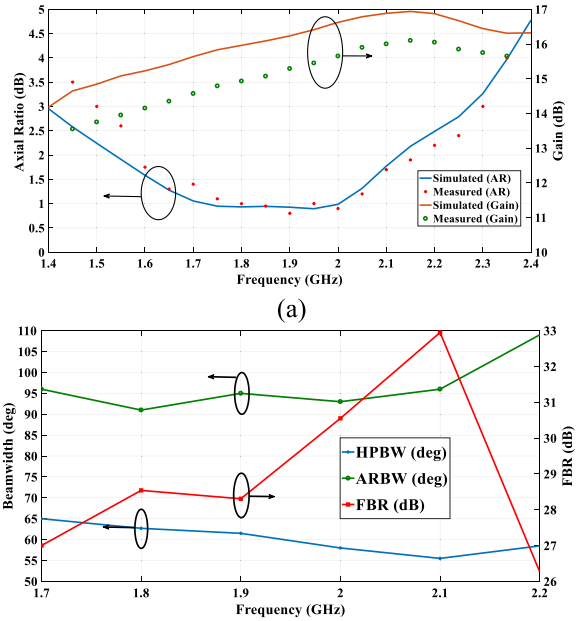


**FIGURE 18.** (a) Simulated and measured axial ratio and gain of the 8-element antenna array. (b) Simulated HPBW, ARBW, and FBR of the 8-element antenna array.

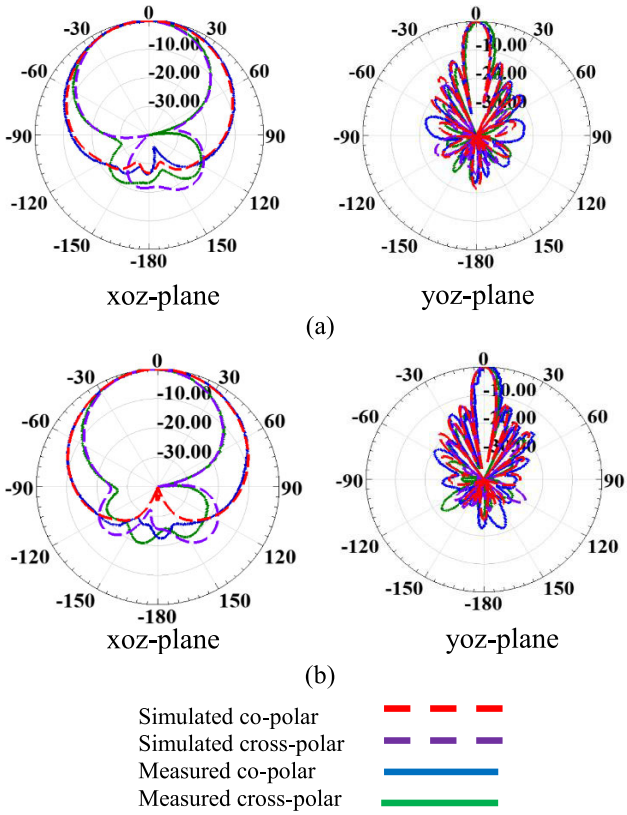


**FIGURE 19.** Radiation patterns of the 8-element antenna array at (a) 1.7 GHz, and (b) 1.9 GHz.

## VII. CONCLUSION

This paper presents a broadband CP fan-shaped crossed-dipole antenna with a pair of three-quarter circular phase

shifters and two different types of parasitic elements. Phase shifters play a principal role in the propagation of LHCP waves as generators of sequential phases. It is possible to achieve a high degree of circular polarization purity and enhance the operational AR bandwidth of the antenna using parasitic elements. The experimental results confirm that the proposed antenna achieves an impedance bandwidth of 57% (1.47-2.65 GHz) for VSWR $< 2$, a 3 dB AR bandwidth of 33% (1.65-2.3 GHz), and a peak gain of 8.7 dB. A 4-element array with impedance and 3 dB AR bandwidths of 66% and 39% and an 8-element array with impedance and 3 dB AR bandwidths of (56% and 12.6%) and 42% were implemented using the proposed CP dipole antenna and tested to demonstrate their potential as cellular base station antennas for covering PCS/DCS/UMTS applications. According to the experimental far-field results of the proposed arrays, the HPBWs, ARBWs, FBRs, and peak gains were $64°\pm 3°$, $> 90°$, $> 25$ dB, 13.2, and 16.1 dB, respectively.

## REFERENCES

[1] X. Zhang, G. Yang, X. Wang, and B. Li, "A dual-band and dual-polarized antenna array for 2G/3G/LTE base stations," *Int. J. RF Microw. Comput.-Aided Eng.*, vol. 26, no. 2, pp. 154–163, Oct. 2015, doi: 10.1002/mmce.20948.

[2] H. Huang, Y. Liu, and S. Gong, "A novel dual-broadband and dual-polarized antenna for 2G/3G/LTE base stations," *IEEE Trans. Antennas Propag.*, vol. 64, no. 9, pp. 4113–4118, Sep. 2016, doi: 10.1109/TAP.2016.2589966.

[3] Y. He, W. Tian, and L. Zhang, "A novel dual-broadband dual-polarized electrical downtilt base station antenna for 2G/3G applications," *IEEE Access*, vol. 5, pp. 15241–15249, 2017, doi: 10.1109/ACCESS.2017.2720591.

[4] L. Ye, G. Liu, Y. Li, J. Li, Z. Hu, and D. Wu, "Broadband dual-polarized crossed-dipole antenna with tapered integrated balun for base-station applications," *Int. J. RF Microw. Comput. Eng.*, vol. 31, no. 7, pp. 1–11, Apr. 2021, doi: 10.1002/mmce.22687.

[5] S. Fu, Z. Cao, P. Chen, D. Gao, and X. Quan, "A novel bandwidth-enhanced dual-polarized antenna with symmetrical closed-resonant-slot pairs," *IEEE Access*, vol. 7, pp. 87943–87950, 2019, doi: 10.1109/ACCESS.2019.2925389.

[6] Q. X. Chu, D. L. Wen, and Y. Luo, "A broadband $\pm 45°$ dual-polarized antenna with Y-shaped feeding lines," *IEEE Trans. Antennas Propag.*, vol. 63, no. 2, pp. 483–490, Feb. 2015, doi: 10.1109/TAP.2014.2381238.

[7] Y. Cui, L. Wu, and R. Li, "Bandwidth enhancement of a broadband dual-polarized antenna for 2G/3G/4G and IMT base stations," *IEEE Trans. Antennas Propag.*, vol. 66, no. 12, pp. 7368–7373, Dec. 2018, doi: 10.1109/TAP.2018.2867046.

[8] Z. Bao, Z. Nie, and X. Zong, "A novel broadband dual-polarization antenna utilizing strong mutual coupling," *IEEE Trans. Antennas Propag.*, vol. 62, no. 1, pp. 450–454, Jan. 2014, doi: 10.1109/TAP.2013.2287010.

[9] Y. Gou, S. Yang, J. Li, and Z. Nie, "A compact dual-polarized printed dipole antenna with high isolation for wideband base station applications," *IEEE Trans. Antennas Propag.*, vol. 62, no. 8, pp. 4392–4395, Aug. 2014, doi: 10.1109/TAP.2014.2327653.

[10] Y. Huo, K. Zhang, C. Guo, H. Zhai, and Y. Zeng, "A compact multimode broadband dual-polarized base station antenna for LTE and 5G applications," *Int. J. RF Microw. Comput.-Aided Eng.*, vol. 31, no. 5, pp. 1–10, Feb. 2021, doi: 10.1002/mmce.22598.

[11] B. Li, Y.-Z. Yin, W. Hu, Y. Ding, and Y. Zhao, "Wideband dual-polarized patch antenna with low cross polarization and high isolation," *IEEE Antennas Wireless Propag. Lett.*, vol. 11, pp. 427–430, 2012, doi: 10.1109/LAWP.2012.2195149.

[12] Y. Gou, S. Yang, Q. Zhu, and Z. Nie, "A compact dual-polarized double E-shaped patch antenna with high isolation," *IEEE Trans. Antennas Propag.*, vol. 61, no. 8, pp. 4349–4353, Aug. 2013, doi: 10.1109/TAP.2013.2262664.

[13] J.-F. Li, D.-L. Wu, G. Zhang, Y.-J. Wu, and C.-X. Mao, "Compact dual-polarized antenna for dual-band full-duplex base station applications," *IEEE Access*, vol. 7, pp. 72761–72769, 2019, doi: 10.1109/ACCESS.2019.2918982.

[14] F. Ghaedi, J. Jamali, and M. Taghizadeh, "A wideband dual-polarized antenna using magneto-electric dipoles for base station applications," *AEU-Int. J. Electron. Commun.*, vol. 126, Nov. 2020, Art. no. 153395, doi: 10.1016/j.aeue.2020.153395.

[15] L. Siu, H. Wong, and K.-M. Luk, "A dual-polarized magneto-electric dipole with dielectric loading," *IEEE Trans. Antennas Propag.*, vol. 57, no. 3, pp. 616–623, Mar. 2009, doi: 10.1109/TAP.2009.2013430.

[16] L. Pollayi, R. K. Dasari, and V. M. Pandharipande, "Design and development of wide band dual-polarized magneto electric dipole antenna for mobile communications," *Int. J. Microw. Wireless Technol.*, vol. 11, no. 2, pp. 175–181, Mar. 2019, doi: 10.1017/S1759078718001642.

[17] Y. Liu, S. Wang, X. Wang, and Y. Jia, "A differentially fed dual-polarized slot antenna with high isolation and low profile for base station application," *IEEE Antennas Wireless Propag. Lett.*, vol. 18, no. 2, pp. 303–307, Feb. 2019, doi: 10.1109/LAWP.2018.2889645.

[18] S. X. Ta, I. Park, and R. W. Ziolkowski, "Crossed dipole antennas: A review," *IEEE Antennas Propag. Mag.*, vol. 57, no. 5, pp. 107–122, Oct. 2015, doi: 10.1109/MAP.2015.2470680.

[19] T. T. Le and H. H. Tran, "Dual-band dual-sense circularly polarized antenna based on crossed dipole structure for WLAN/WiMAX applications," *Int. J. RF Microw. Comput.-Aided Eng.*, vol. 29, no. 10, pp. 1–8, Jun. 2019, doi: 10.1002/mmce.21866.

[20] S. X. Ta, I. Park, and R. W. Ziolkowski, "Circularly polarized crossed dipole on an HIS for 2.4/5.2/5.8-GHz WLAN applications," *IEEE Antennas Wireless Propag. Lett.*, vol. 12, pp. 1464–1467, 2013, doi: 10.1109/LAWP.2013.2288787.

[21] F.-P. Lai, J.-F. Yang, and Y.-S. Chen, "Compact dual-band circularly polarized antenna using double cross dipoles for RFID handheld readers," *IEEE Antennas Wireless Propag. Lett.*, vol. 19, no. 8, pp. 1429–1433, Aug. 2020, doi: 10.1109/LAWP.2020.3004881.

[22] S. Bhaskar and A. K. Singh, "Linearly tapered meander line cross dipole circularly polarized antenna for UHF RFID tag applications," *Int. J. RF Microw. Comput.-Aided Eng.*, vol. 29, no. 5, Oct. 2018, Art. no. e21563, doi: 10.1002/mmce.21563.

[23] C. Bajaj, D. K. Upadhyay, S. Kumar, and B. K. Kanaujia, "Compact circularly polarized cross dipole antenna for RFID handheld readers/IoT applications," *AEU-Int. J. Electron. Commun.*, vol. 155, Oct. 2022, Art. no. 154343, doi: 10.1016/j.aeue.2022.154343.

[24] Z.-Y. Zhang, S. Zuo, Y. Zhao, L.-Y. Ji, and G. Fu, "Broadband circularly polarized bowtie antenna array using sequentially rotated technique," *IEEE Access*, vol. 6, pp. 12769–12774, 2018, doi: 10.1109/ACCESS.2018.2802938.

[25] R. Xu, J.-Y. Li, and W. Kun, "A broadband circularly polarized crossed-dipole antenna," *IEEE Trans. Antennas Propag.*, vol. 64, no. 10, pp. 4509–4513, Oct. 2016, doi: 10.1109/TAP.2016.2588523.

[26] M. Pourbagher, J. Nourinia, and C. Ghobadi, "Circularly polarized printed crossed-dipole antenna using branch-line feed network for GPS applications," *AEU-Int. J. Electron. Commun.*, vol. 120, Jun. 2020, Art. no. 153226, doi: 10.1016/j.aeue.2020.153226.

[27] W. He, Y. He, Y. Li, S.-W. Wong, and L. Zhu, "A compact ultrawideband circularly polarized antenna array with shared partial patches," *IEEE Antennas Wireless Propag. Lett.*, vol. 20, no. 12, pp. 2280–2284, Dec. 2021, doi: 10.1109/LAWP.2021.3107218.

[28] J. Fan, J. Lin, J. Cai, and F. Qin, "Ultra-wideband circularly polarized cavity-backed crossed-dipole antenna," *Sci. Rep.*, vol. 12, no. 1, pp. 1–10, Mar. 2022, doi: 10.1038/s41598-022-08640-z.

[29] A. Kumar, A. A. Althuwayb, D. Chaturvedi, R. Kumar, and F. Ahmadfard, "Compact planar magneto-electric dipole-like circularly polarized antenna," *IET Commun.*, vol. 16, no. 20, pp. 2448–2453, Sep. 2022, doi: 10.1049/cmu2.12499.

[30] N. Jaglan, S. D. Gupta, B. K. Kanaujia, and M. S. Sharawi, "10 element sub-6-GHz multi-band double-T based MIMO antenna system for 5G smartphones," *IEEE Access*, vol. 9, pp. 118662–118672, 2021, doi: 10.1109/ACCESS.2021.3107625.

[31] N. Jaglan, S. D. Gupta, and M. S. Sharawi, "18 element massive MIMO/diversity 5G smartphones antenna design for sub-6 GHz LTE bands 42/43 applications," *IEEE Open J. Antennas Propag.*, vol. 2, pp. 533–545, 2021, doi: 10.1109/OJAP.2021.3074290.

[32] D. Chaturvedi and A. Kumar, "A QMSIW cavity-backed self-diplexing antenna with tunable resonant frequency using CSRR slot," *IEEE Antennas Wireless Propag. Lett.*, vol. 23, no. 1, pp. 259–263, Jan. 2024, doi: 10.1109/LAWP.2023.3323008.
[33] C. A. Balanis, *Antenna Theory: Analysis and Design*. Hoboken, NJ, USA: Wiley, 2016.

**MEHDI SEFIDI** was born in Miandoab, Iran, in 1980. He received the B.Sc. degree in telecommunications engineering from IAU University, Urmia, West Azerbaijan, Iran, in 2005, and the M.Sc. degree from IAU South Tehran Branch, in 2009. He is currently pursuing the Ph.D. degree in electrical telecommunication field and wave with Urmia University, Urmia. His research interests include circularly polarized antenna arrays, MIMO antenna design and miniaturization, reconfigurable antennas, multiband antennas, wireless local-area network antennas, and UWB systems.

**CHANGIZ GHOBADI** received the B.Sc. degree in electrical engineering and the M.Sc. degree in electrical engineering telecommunication from the Isfahan University of Technology, Isfahan, Iran, and the Ph.D. degree in electrical telecommunication from the University of Bath, Bath, U.K., in 1998. He is currently a Professor with the Department of Electrical Engineering, Urmia University, Iran. He has supervised and administered a thesis for over 130 M.Sc. and 32 Ph.D. students. He has authored or coauthored more than 360 scientific publications, including accredited journals and conferences. His articles have been cited more than 5750 times. His current research interests include antenna design, radar, and adaptive filters. Thomson Reuters listed him as one of the top 1% of the world's scientists and academics, in 2017, 2020, and 2022.

**JAVAD NOURINIA** (Senior Member, IEEE) received the B.Sc. degree in electrical and electronic engineering from Shiraz University, the M.Sc. degree in electrical and telecommunication engineering from the Iran University of Science and Technology, and the Ph.D. degree in electrical and telecommunication from the University of Science and Technology, Tehran, Iran, in 2000. He was the Head of the Faculty of Engineering, from 2013 to 2017. His research interests include small antennas, filters, periodic structures, and optimization. Since 2016, Thomson Reuters listed him as one of the top 1% of the world's scientists and academics.

**RAHIM NADERALI** was born in Urmia, Iran, in 1963. He received the B.Sc. degree in physics from Urmia University, Urmia, in 1990, the M.Sc. degree from Tabriz University, in 1992, and the Ph.D. degree from Urmia University, in 2010. He is currently an Associate Professor with Urmia University.